Composition and growth of thin anodic oxides on InP(100)

Djenizian, T.; Sproule, G. I.; Moisa, S.; Landheer, D.; Wu, X.; Santinacci, L.; Schmuki, P.; Graham, M. J.

Publisher's version / Version de l'éditeur:
https://doi.org/10.1016/S0013-4686(02)00138-X
Electrochimica acta, 47, 17, pp. 2733-2740, 2002-07-05

PERGAMON

Electrochimica Acta 47 (2002) 2733–2740

ELECTROCHIMICA Acta

www.elsevier.com/locate/electacta

Composition and growth of thin anodic oxides formed on InP (100)

T. Djenizian [a], G.I. Sproule [b], S. Moisa [b], D. Landheer [b], X. Wu [b], L. Santinacci [a], P. Schmuki [a,*], M.J. Graham [b]

[a] *Department of Material Science, LKO, University of Erlangen-Nuremberg, Martensstr. 7, D-91058 Erlangen, Germany*
[b] *Institute for Microstructural Sciences, National Research Council of Canada, Ottawa, Canada K1A 0R6*

Received 22 November 2001; received in revised form 5 March 2002

Abstract

Thin anodic oxides (< 100 Å) were formed on p-InP (100) in phosphate solution (0.3 M $NH_4H_2PO_4$) and in sodium tungstate solution (0.1 M $Na_2WO_4 \cdot 2H_2O$) at different temperatures (25 and 80 °C) and potentials (1–8 V). Thickness and composition were determined by different surface-analytical techniques including Auger electron spectroscopy, X-ray photoelectron spectroscopy, scanning electron microscopy, atomic force microscopy and transmission electron microscopy. In general, it has been observed that double-layered films are obtained with an outer In-rich layer. The thickness of the outer layer, oxide morphology and roughness as well as the composition of the duplex structure are strongly dependent on the temperature and the composition of the electrolyte. It has been found that oxides formed in phosphate exhibit a higher stability against dissolution compared with oxides formed in tungstate. The latter contain a large amount of In_2O_3, which leads to poor electrical properties.

Keywords: Anodic oxide; InP; Surface analysis; Double-layered films; Electrical properties

1. Introduction

Due to their direct band gap III–V, semiconductor compounds such as GaAs and InP have been the subject of a large number of investigations to fabricate a variety of devices used for optical communication and high-speed electronic systems. In order to develop these technologies, oxidation of III–V compounds, in particular GaAs, has been extensively studied [1–3] with emphasis on surface-analytical techniques [4–6]. Investigations have also focused on InP, an attractive candidate for a wide range of applications. Various devices using InP have been fabricated including metal–insulator–semiconductor field effect transistors (MIS-FETs), photo-electrochemical solar cells [7], light emitting diodes [8] and components for optical fiber communications [9]. But in contrast to Si, the thermal oxide formed on InP is of low quality and tends to be too conductive for use as a gate insulator.

In comparison with thermal oxidation, anodic oxidation results in a significant improvement in electrical properties. Anodic layers can be grown on InP using both aqueous (0.1 N KOH) [10] and non-aqueous (0.1 N sodium salicylate in ethanol) electrolytes [11]. Results reported have shown improved oxides in terms of resistivity, but in all cases high leakage currents have been observed limiting the field of application. Investigations dealing with anodic oxides formed in electrolytes such as AGW (a mixed solution of glycol and water) and sodium tungstate (0.1 M $Na_2WO_4 \cdot 2H_2O$) have also been reported [12–17].

In the present work, the composition and growth of anodic oxide films are studied in sodium tungstate and phosphate solutions at different temperatures. The influence of the potential and temperature on the chemical composition and thickness of the oxides was studied by Auger electron spectroscopy (AES) and X-ray photoelectron spectroscopy (XPS) complemented by transmission electron microscopy (TEM). The oxide morphology has been assessed by scanning electron microscopy (SEM) and atomic force microscopy

* Corresponding author. Fax: +49-91318527582.
E-mail address: schmuki@ww.uni-erlangen.de (P. Schmuki).

0013-4686/02/$ - see front matter
PII: S0013-4686(02)00138-X

(AFM). Electrical measurements were performed on metal–insulator–semiconductor (MIS) structures.

2. Experimental

Experiments were carried out on p-InP (100) doped with $\sim 3.5 \times 10^{18}$ Zn atoms/cm^3. The samples were cleaved, degreased by sonicating in C_3H_6O, isopropanol and MeOH, rinsed with de-ionized water and dried in an Ar stream. Subsequently the samples were immersed in 1% HF for 1 min to remove the air formed film.

Contact to the InP was established by scratching InGa eutectic on the backside of the sample. The electrochemical set-up consisted of a conventional three-electrode configuration with a Pt gauze as a counter electrode and a Haber–Luggin capillary with a Ag/AgCl electrode as a reference electrode. Electrochemical experiments were carried out using an EG&G 173 potentiostat. Anodic polarization curves with a step size of 10 mV/s were acquired in 0.1 M $Na_2WO_4 \cdot 2H_2O$ electrolyte (pH 8.2) and in 0.3 M $NH_4H_2PO_4$ electrolyte (pH 4.4) at different temperatures (25 and 80 °C). The solutions were prepared from analytical grade chemicals and de-ionized water. Potential step experiments were carried out at three different anodic potentials (1, 4 and 8 V/(Ag/AgCl)) for 5 min in phosphate and tungstate solutions.

Chemical characterization of oxides was carried out by AES using a PHI 650 system. XPS analysis was performed in a PHI 5500 system equipped with an Al K_α monochromatic source and an analyzer pass energy of 11.75 eV for high resolution spectra to obtain chemical state information. For XPS, the samples were Ar^+ sputtered for 5 min (at a rate $\sim$1–2 Å/min) to eliminate adventitious carbon contamination. Also, the take-off angle (of the sample with respect to the analyzer) was set at 70° to enhance the signal from components closer to the substrate interface. The reference used was the O 1s binding energy, BE = 531.85 eV for the sputtered samples, with respect to the C 1s BE = 285.0 eV before sputtering. TEM measurements were performed with a Philips EM 430T operating at 250 keV; cross sectional samples were made by ion milling. SEM examination was carried out using a Hitachi S-4700 FESEM, and AFM with a Digital Instruments Nanoscope III.

Electrical measurements were performed on MIS structures. After deposition of Al dots (area of 6×10^{-4} cm^2), the samples were annealed in forming gas (4% H_2 in N_2) at 350 °C for 20 min. Back contacts were made with eutectic InGa and the current–voltage characteristics were obtained with a probe station and a Hewlett–Packard Model 4140B picommeter/DC voltage source.

3. Results and discussion

3.1. Electrochemical measurements

Fig. 1 shows anodic polarization curves from −0.5 to 5 V (Ag/AgCl) for p-InP in sodium phosphate and tungstate solutions at 25 and 80 °C. For all samples, there are two distinct regions: at low anodic potential, log i is approximately proportional to V and corresponds to an active dissolution range. At distinct potentials a maximum occurs (an active–passive transition) with nucleation and growth of oxides and at potentials higher than approximately 1 V the current density reaches a constant value. This steady state, characterized by a current density independent of the voltage, can be attributed to the balance between growth and dissolution of the oxide film. The composition of the electrolyte has an influence on the electrochemical behavior. In phosphate at 25 °C (Fig. 1a) the active–passive transition occurs at a lower current density than in tungstate (Fig. 1c) suggesting a facilitated growth of the oxide in the phosphate buffer, and the steady state current density is lower suggesting a higher quality passive film. Temperature also plays a crucial role: oxidation kinetics are clearly enhanced by increased temperature as illustrated by a higher current density at low anodic potential (Fig. 1d) compared with data at 25 °C (Fig. 1c).

3.2. AES profiles

AES depth profiles reveal that the anodic films grown in both solutions at different temperatures are duplex in nature. As has been previously reported [18–20], the formation of a two-layered film is often observed, consisting of an outer layer rich in In and an inner

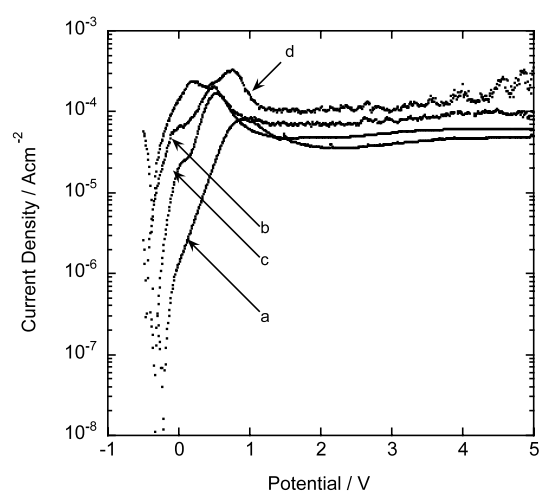

Fig. 1. Anodic polarization curves from −0.5 to 5 V (Ag/AgCl) for p-InP (100) in 0.3 M $NH_4H_2PO_4$ at 25 (a), 80 °C (b) and in 0.1 M $Na_2WO_4 \cdot 2H_2O$ at 25 (c), 80 °C (d). The step size was 10 mV/s.

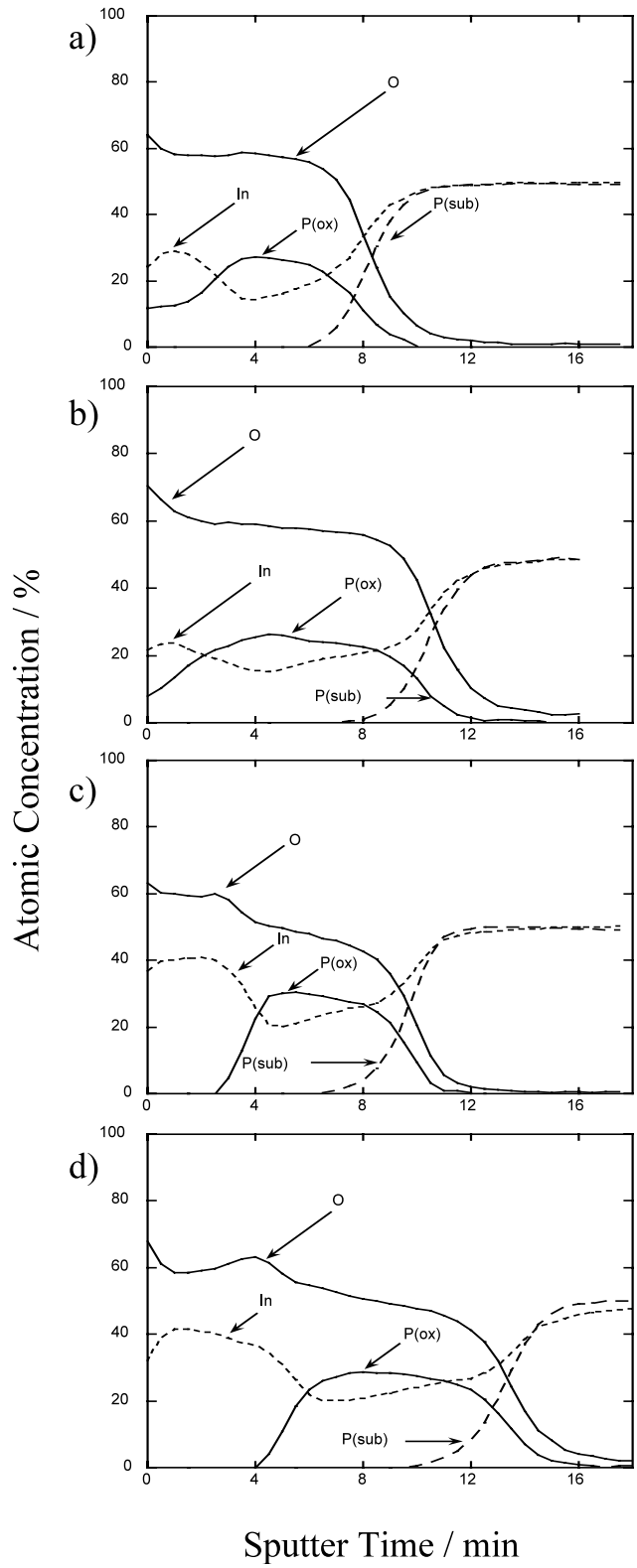

Fig. 2. AES profiles of the anodic films formed on InP (100) at 8 V (Ag/AgCl) for 5 min in 0.3 M $NH_4H_2PO_4$ at 25 (a), 80 °C (b) and in 0.1 M $Na_2WO_4 \cdot 2H_2O$ at 25 (c), 80 °C (d). Sputtering was by 1 keV argon ions.

layer containing both In and P as shown by the profiles in Fig. 2. The existence of the two-layered film could be explained by the fact that P^{5+}–O bonds (424 kJ/mol) are stronger than In^{3+}–O bonds (181 kJ/mol) and hence In^{3+} cations have a greater mobility through the film during anodizing. Therefore, an In-rich layer is grown at the surface while P^{5+} cations are mainly present in the inner layer. Regarding the AES depth profile obtained in tungstate at 25 °C (Fig. 2c), the outer layer contains only In and O, and P is confined strictly to the inner oxide film. A similar AES depth profile is obtained for the sample anodized at higher temperature (Fig. 2d), although the interfaces (outer layer–inner layer and inner layer–substrate) are somewhat broadened. The increased thickness of the In-rich layer supports the literature data of a higher mobility of indium species compared with phosphorus species. For oxides formed in phosphate at 25 (Fig. 2a) and 80 °C (Fig. 2b) the AES depth profiles indicate that the films are more homogeneous in terms of composition. While the film appears to be two-layered, the outer layer contains significant phosphorus species. It can be noted that the thickness of the outer layer is not affected by the high temperature treatment although the substrate–oxide interface is broadened. The concentration of phosphorus is higher in the outer region with the phosphate electrolyte, possibly due to the incorporation of species provided by the electrolyte and/or to a weaker etching of phosphorus-containing species. In the AES profiles, the sensitivity factors of In and P in the substrate have been adjusted such that the both concentrations approach 50 at.%. The Auger peak shape for phosphorus in the oxide is significantly different from that in the bulk, requiring different sensitivity factors for phosphorus in the oxide. Thus the elemental concentrations for the oxide are only approximate. Similar AES profiles (not shown) are obtained for samples anodized at less positive potentials under the same conditions and reveal the influence of the electrolyte composition on oxide film growth rate. The growth rate tends to be higher in tungstate ($\sim$6 Å/V) compared with phosphate solution ($\sim$3 Å/V) as shown in Fig. 3, where it is observed that the oxide thickness varies linearly with the applied potential under the different conditions. Hence, increased temperature does not drastically affect the thickness of the films suggesting an increased etching of oxide species.

3.3. XPS analysis

In order to investigate in more detail the composition of the inner oxide film, XPS analysis was performed on the samples used for AES depth profile experiments, which were sputtered until the phosphorus-containing film region was revealed. The resultant O 1s, P 2p and In $3d_{5/2}$ spectra of the sample anodized for 5 min at 8 V in phosphate ($T = 25$ °C) are presented in Fig. 4. Various species are probably present in the phosphorus-rich layer including oxides like In_2O_3 and P_2O_5 and phos-

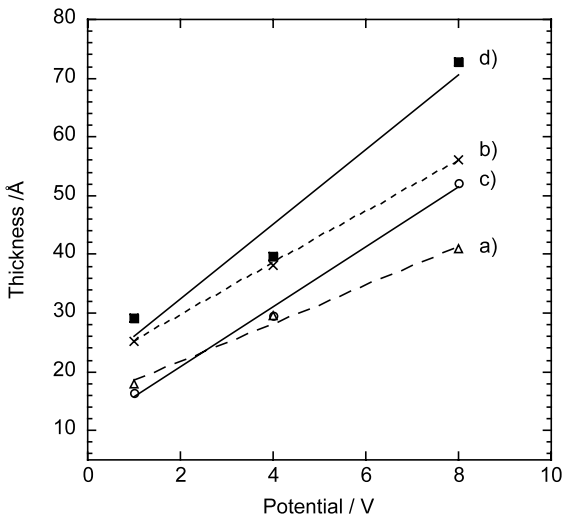

Fig. 3. Variation of oxide thickness with applied voltage. Anodic potential was applied for 5 min in 0.3 M $NH_4H_2PO_4$ at 25 (a), 80 °C (b) (dashed lines) and in 0.1 M $Na_2WO_4 \cdot 2H_2O$ at 25 (c), 80 °C (d) (solid lines). Oxide thickness were determined from the sputter time in the AES profile when the oxygen signal fell to 50%; sputter times were calibrated by TEM measurements of oxide thickness (cf. Fig. 7).

phate and polyphosphate compounds $InPO_4$, $In(PO_3)_3$ and $In(PO_y)_x$ [21] with x approximately equal to 3 and y in the range 3–5 [22]. Curve-fitting was performed using the binding energies of Hollinger et al. [4,23] and Faur et al. [24]. Curve-fitting of the In $3d_{5/2}$ signal (Fig. 4a) reveals that the inner layer is composed of $In(PO_y)_x$, $InPO_4$ and/or $In(PO_3)_3$ and In_2O_3. As the peak related to $InPO_4$ and $In(PO_3)_3$ occurs at a similar energy it is not possible to specify if one or both species are present in the film. The yield corresponding to the latter two species is significantly greater than the yield from In_2O_3 and $In(PO_y)_x$ indicating that one or two of these species dominate. Curve-fitting of the P 2p peak (Fig. 4b) is consistent with the In $3d_{5/2}$ data. Peaks corresponding to $InPO_4$ and $In(PO_3)_3$ and $In(PO_y)_x$ and/or P_2O_5 species are clearly identified. The relative yields indicate a large dominance of $InPO_4$ and $In(PO_3)_3$ over other phosphorus-containing species. Similarly, the curve-fitting of the O 1s peak (Fig. 4c) supports the significantly greater presence of $InPO_4$ and/or $In(PO_3)_3$. The contributions of In_2O_3 and $In(PO_y)_x$ and/or P_2O_5 are small. Fig. 5 shows the curve-fitting for the In $3d_{5/2}$ peak for samples treated under different conditions (curve-fitting for other ele-

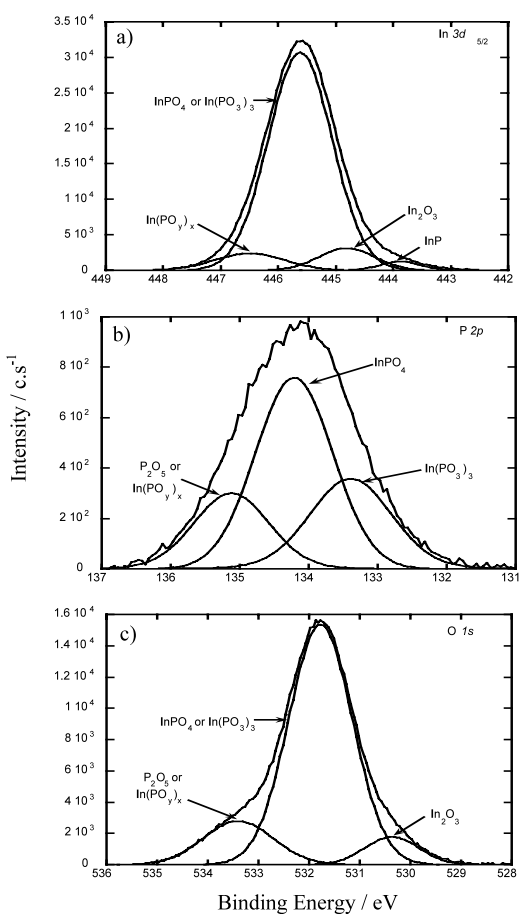

Fig. 4. Deconvoluted In $3d_{5/2}$ (a) P 2p (b) and O 1s (c) XPS spectra of the oxide formed at 8 V (Ag/AgCl) for 5 min in 0.3 M $NH_4H_2PO_4$ at 25 °C.

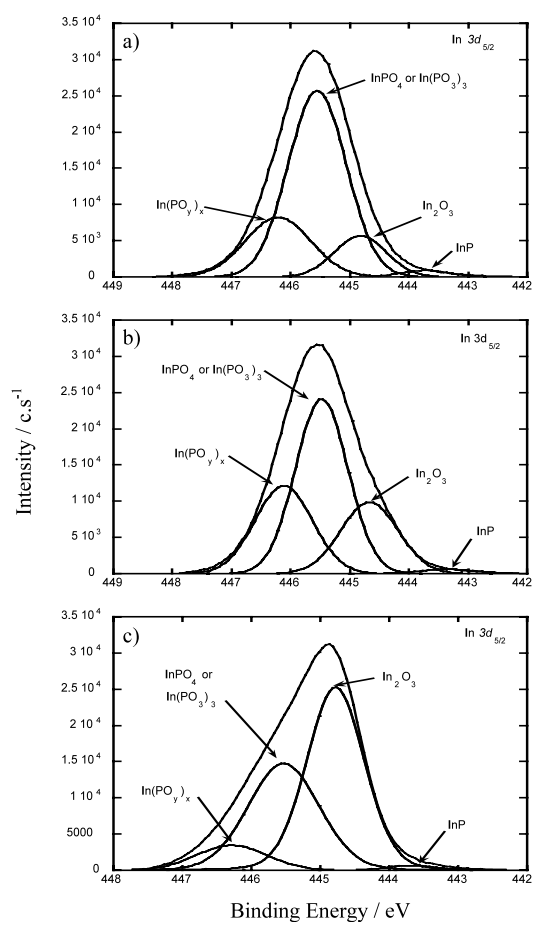

Fig. 5. Deconvoluted In $3d_{5/2}$ XPS spectra of the oxides formed at 8 V (Ag/AgCl) for 5 min in 0.3 M $NH_4H_2PO_4$ at 80 °C (a), in 0.1 M $Na_2WO_4 \cdot 2H_2O$ at 25 (b) and 80 °C (c).

ments are not shown but are consistent). The oxide formed in phosphate at 80 °C (Fig. 5a) shows a little more $In(PO_y)_x$ and In_2O_3 than at 25 °C (Fig. 4a). The oxide obtained in sodium tungstate solution at 25 °C (Fig. 5b) shows that $InPO_4$ and/or $In(PO_3)_3$ species are less predominant in the phosphorus-rich layer due to contributions from both $In(PO_y)_x$ and In_2O_3. The increased quantity of In_2O_3 is certainly due to a greater stability of the compound in this electrolyte. Indeed, according to the literature [25], In_2O_3 is thermodynamically stable at pH 8.2, therefore it can be formed easily in tungstate solution, particularly at 80 °C (Fig. 5c). Using phosphate (pH 4.4) at $T = 25$ °C does not lead to stable In_2O_3, and therefore a smaller quantity is detected by XPS (Fig. 4a). Furthermore, the significant presence of In_2O_3 for oxide formed in tungstate could also be explained by the fact that adsorption of electrolyte compounds at the surface can play a role in determining the oxide film composition. It can be noted that tungsten-species (not shown) are observed in the outer regions of the film. Previous XPS work indicated that these species are present as $(WO_4)^{2-}$ and/or WO_3 [17]. Consequently, it is assumed that in phosphate solution phosphorus-species adsorbed at the surface are able to be integrated into the oxide film and react with In species leading to an increased yield of polyphosphates and a decrease of In_2O_3.

The different concentrations of species can therefore be explained in terms of the stability and solubility of the compounds involved depending on both temperature and electrolyte composition. Indeed, the solubility of phosphate and polyphosphate is greater than oxide and increases with temperature. Phosphate and polyphosphate species are more stable in phosphate solution at the different temperatures. In tungstate solution, In_2O_3 is more stable than phosphorus-containing species, which are likely easily removed. Furthermore, In_2O_3 is more stable at the higher temperature. Regarding anodic oxide growth, a film composed of units of In_2O_3 and P_2O_5, as pointed out previously [22,26] can be explained in terms of formation of anodic films on alloy substrates, developed for aluminum alloys [27]. Thus, indium and phosphorus are oxidized at the substrate–film interface to form In^{3+} and P^{5+} ions within an oxide composed of units of In_2O_3 and P_2O_5. The former ions are more mobile in the growing oxide film and hence, an outer layer of amorphous In_2O_3 develops above the inner layer by growth at the film–electrolyte interface. The inner layer is phosphorus-rich due to loss of the In^{3+} ions to the outer layer. O^{2-} ions migrate inward through the outer and inner amorphous layer, resulting in the formation of P_2O_5, $InPO_4$ and $In(PO_3)_3$ species at the substrate–film interface. The mechanism of oxidation is modeled in more detail in Ref. [22].

3.4. Oxide morphology

SEM examination of the anodic film formed at 8 V for 5 min in phosphate (25 °C) reveals a uniform

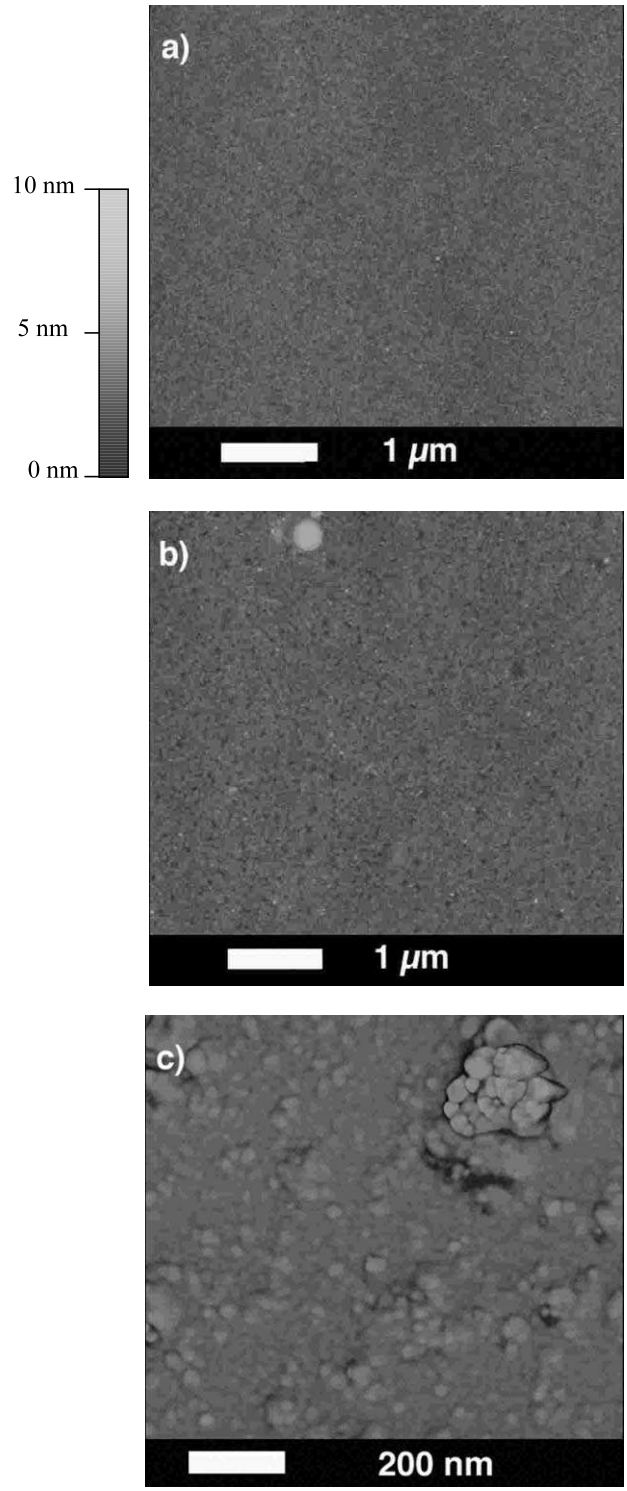

Fig. 6. AFM images in plan view of oxide formed at 8 V (Ag/AgCl) for 5 min in 0.3 M $NH_4H_2PO_4$ at 25 °C (a), in 0.1 M $Na_2WO_4 \cdot 2H_2O$ at 80 °C (b), and of some island areas present in oxides formed in tungstate at 80 °C (c). The z-scale is 10 nm.

texture and a relatively low roughness. Tapping-mode AFM (Fig. 6a) confirms that the typical feature sizes are in the 100 Å range and the root mean square (RMS) roughness is found to be ~3 Å. The coalescence of the oxide grains leads to a remarkably smooth film. Anodizing in tungstate (8 V, 80 °C) shows a less homogeneous texture due to the presence of particles (~3000 Å diameter) and what appear to be islands dispersed through the continuous film. Fig. 6b shows the AFM image of the uniform area; typical grain sizes in the 400 Å range lead to a RMS roughness of ~4 Å. AES analysis performed in the different regions show the particles and islands to be composed of In, O and P and the homogeneous region to contain no phosphorus suggesting the formation of In_2O_3. Fig. 6c shows the phase-mode AFM image of the islands which reveals that they are composed of grain sizes in the 400 Å range (the RMS roughness is ~70 Å). It should be noted that few islands are also observed on samples anodized in phosphate at 80 °C and in tungstate at 25 °C.

TEM cross sections confirm rougher surfaces for oxides formed in tungstate 80 °C (Fig. 7a). The rougher substrate–film interface would also suggest that oxide formed in tungstate at high temperature might have poor electrical properties. Fig. 7b shows the TEM image of oxide film formed in phosphate at 80 °C. Clearly the film appears more homogenous and smoother than the film formed in tungstate solution.

3.5. Electrical measurements

Electrical measurements were performed on MIS structures. Samples anodized in tungstate at 80 °C exhibited a high leakage current, likely the result of the low quality of the oxide–substrate interface leading to a high density of electronic traps combined with a large amount of conductive In_2O_3. Anodic oxide (~40 Å thick) formed in phosphate solution at 25 °C showed improved electrical properties. Fig. 8 shows the variation of the current density as a function of the gate bias. As shown in the inset, the current rises in a piecewise linear fashion between −1.6 and −3.7 V, characteristic of ionic or electronic ohmic conduction processes. At a gate potential of −4.5 V the current density rises rapidly to a value >0.01 A/cm^2. This corresponds to a high breakdown field $E_b = 11$ MV/cm. The observed current densities are sufficiently low to be useful for a number of electronic applications and are low enough to obtain the quasi-static capacitance by ramping the applied voltage from 2.5 to −2.5 V at a ramp rate of 0.1 V/s. For a film of thickness, d, the measured insulator capacitance, C, is related to the film dielectric constant, ε, by the relation $C/A = \varepsilon\varepsilon_0/d$, where A is the capacitor area and ε_0 is the permittivity of vacuum. Using the capacitance obtained at a potential of 1.5 V (in inversion where the leakage current is negligible) gives $\varepsilon = 3.3$.

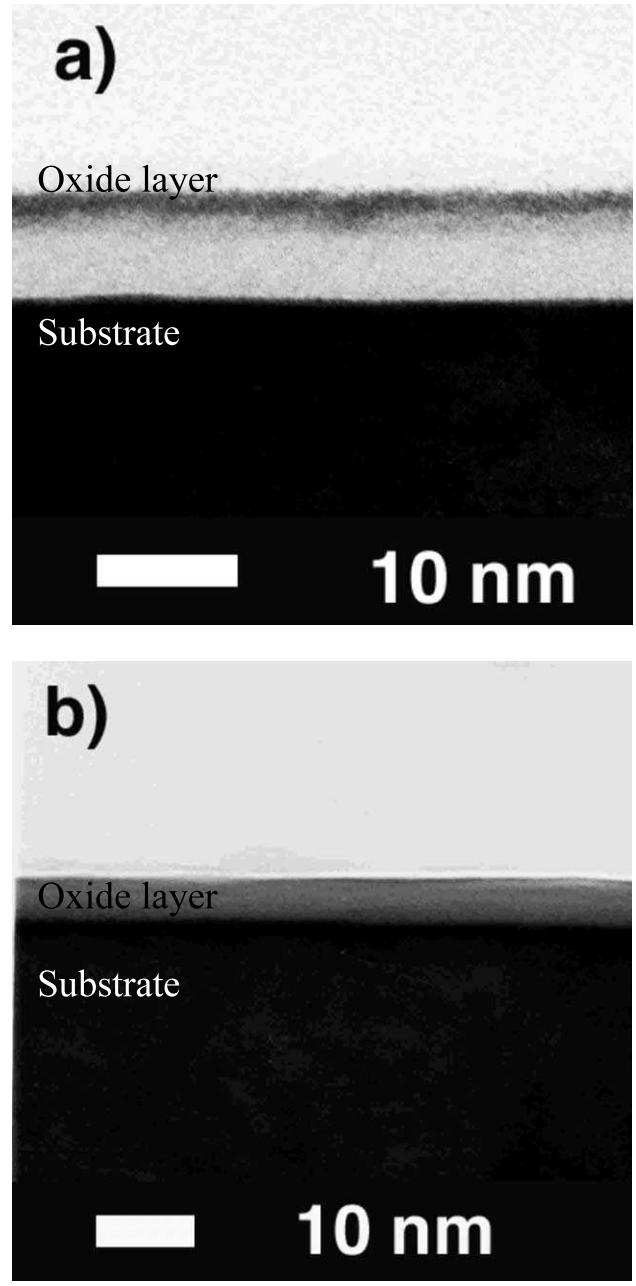

Fig. 7. TEM cross sections produced by ion milling of oxide formed at 8 V (Ag/AgCl) for 5 min in 0.1 M $Na_2WO_4 \cdot 2H_2O$ at 80 °C (a) and in 0.3 M $NH_4H_2PO_4$ at 80 °C (b).

This value is considerably lower than the value $\varepsilon = 68$ reported for indium oxide [28] and is also lower than expected for $InPO_4$. This may be the result of some porosity within the film.

4. Conclusion

Thin anodic oxides (<100 Å) were grown on p-InP (100) in phosphate solution (0.3 M $NH_4H_2PO_4$) and in sodium tungstate solution (0.1 M $Na_2WO_4 \cdot 2H_2O$) at

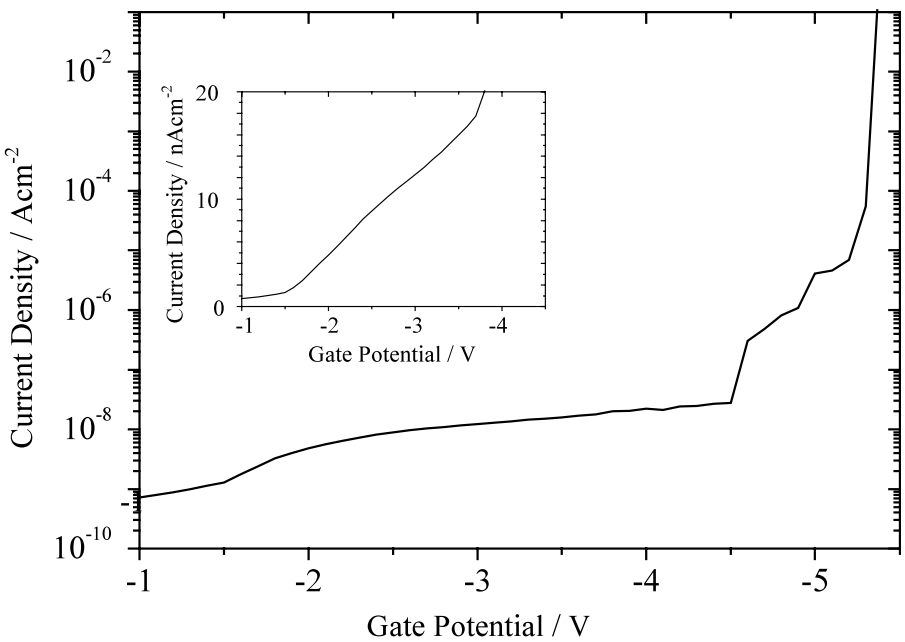

Fig. 8. Variation of current density with gate bias voltage for injection from the gate for ~40 Å thick oxide formed on p-InP (100) anodized at 8 V (Ag/AgCl) for 1 h in 0.3 M $NH_4H_2PO_4$ at 25 °C.

different temperatures (25 and 80 °C). Surface-analytical techniques reveal that the oxide films are composed of a two-layer structure depending on the temperature and the composition of the electrolyte. Due to the film formation mechanism, which involves significant oxide dissolution, high temperature treatment does not lead to dramatically thicker films. It has been found that anodic oxides formed at 8 V for 5 min in tungstate at room temperature and 80 °C show an In_2O_3 outer layer, which is thicker at higher temperature. The texture and the composition of the films are non-uniform. XPS analysis confirms the predominance of In_2O_3, which increases with temperature. The dominance of In_2O_3 could be explained in terms of a greater mobility of indium species though the oxide film and/or a higher solubility of the different phosphorus-containing compounds involved. Oxides formed in phosphate under the same conditions reveal a slower oxide growth rate and a thinner outer layer not significantly varying with temperature. The texture as well as the composition of the films is more uniform and surface analysis shows a predominance of phosphate and polyphosphate species over In_2O_3, suggesting a higher stability of the phosphorus-containing compounds against dissolution. Improved electrical properties have been found for the oxide formed in phosphate because of the low amount of In_2O_3 combined with a higher stability of phosphorus-containing species.

Acknowledgements

The authors thank J.R. Phillips for technical assistance and J.W. Fraser for SEM examination. T.D. thanks J.A. Bardwell for helpful discussions and BMBF for financial support through the Canada/Germany Cooperative R&D Agreement.

References

[1] C.W. Wilmsen, Physics and Chemistry of III–V Compound Semiconductor Interfaces, Plenum, New York, London, 1985.
[2] H. Hasegawa, H.L. Hartnagel, J. Electrochem. Soc. 123 (1976) 713.
[3] C.W. Fischer, S.W. Teare, J. Appl. Phys. 67 (1990) 2608.
[4] G. Hollinger, R. Skheyte-Kabani, M. Gendry, Phys. Rev. B 49 (1994) 11.
[5] T. Hishikawa, H. Ikoma, Jpn. J. Appl. Phys. 31 (1992) 3981.
[6] P. Schmuki, G.I. Sproule, J.A. Bardwell, Z.H. Lu, M.J. Graham, J. Appl. Phys. 79 (1996) 7303.
[7] H. Li, S. Pons, J. Electroanal. Chem. 233 (1987) 1.
[8] P.A. Kohl, C. Wolowodiuk, J.F.W. Ostermayer, J. Electrochem. Soc. 130 (1983) 2288.
[9] A. Guivarc'h, H. L'haridon, G. Pelous, G. Hollinger, P. Pertosa, J. Appl. Phys. 55 (1984) 1139.
[10] C.W. Wilmsen, CRC Crit. Rev. Solid-State Sci. 5 (1975) 313.
[11] D.L. Lile, D.A. Collins, Appl. Phys. Lett. 28 (1976) 554.
[12] D.H. Laughlin, C.W. Wilmsen, Appl. Phys. Lett. 37 (1980) 915.
[13] Y. Robach, J. Joseph, E. Bergignat, B. Commere, G. Hollinger, P. Viktorovitch, Appl. Phys. Lett. 49 (1986) 1281.

[14] C.W. Wilmsen, R.W. Kee, J. Vac. Sci. Technol. 15 (1978) 1513.
[15] F. Echeverria, P. Skeldon, G.E. Thompson, H. Habazaki, K. Shimizu, J. Mater. Sci. 36 (2001) 1253.
[16] R.J. Hussey, G.I. Sproule, J.P. McCaffrey, R. Driad, P.J. Poole, D. Landheer, A.J. Sring Thorpe, A. Pakes, F. Echeverria, P. Skeldon, G.E. Thompson, Proc. Oxide Films Symposium, 197th Meeting of the Electrochemical Society, Toronto, Proc. vol. 2000–4, 2000, 317.
[17] A. Pakes, P. Skeldon, G.E. Thompson, R.J. Hussey, S. Moisa, G.I. Sproule, D. Landheer, M.J. Graham, Proc. Ecacia 01, Avignon, France, September 2001.
[18] K.M. Geib, C.W. Wilmsen, J. Vac. Sci. Technol. B 1 (1983) 837.
[19] M. Salvi, P.N. Favennec, H.L. Haridon, G.P. Pelus, Thin Solid Film 87 (1982) 13.
[20] F. Echeverria, PhD Thesis, UMIST, 1999.
[21] H. Ishii, H. Hasegawa, A. Ishii, H. Ohno, Appl. Surf. Sci. 41–42 (1989) 390.
[22] A. Pakes, P. Skeldon, G.E. Thompson, S. Moisa, G.I. Sproule, M.J. Graham, Corros. Sci. (in press).
[23] G. Hollinger, E. Bergignat, J. Joseph, Y. Robach, J. Vac. Sci. Technol. A 1 (1985) 2082.
[24] M. Faur, D.T. Jayne, M. Goradia, Surf. Interface Anal. 15 (1990) 641.
[25] M. Pourbaix, Atlas d'Equilibres Electrochimiques, Gaultier-Villars & Cie, Paris, 1963.
[26] A. Pakes, F. Echeverria, P. Skeldon, G.E. Thompson, J.W. Fraser, J.P. McCaffrey, S. Moisa, H. Habazaki, M.J. Graham, K. Shimizu, Corros. Sci. 43 (2001) 2173.
[27] H. Habazaki, K. Shimizu, P. Skeldon, G.E. Thompson, G.C. Woud, X. Zhou, Trans. Inst. Met. Finish 75 (1997) 18.
[28] D.K. Jain, J.C. Garg, Indian J. Pure Appl. Phys. 18 (1980) 842.